E-ISSN: 2149-7222 (Online)

Journal Cellular Neuroscience and Oxidative Stress

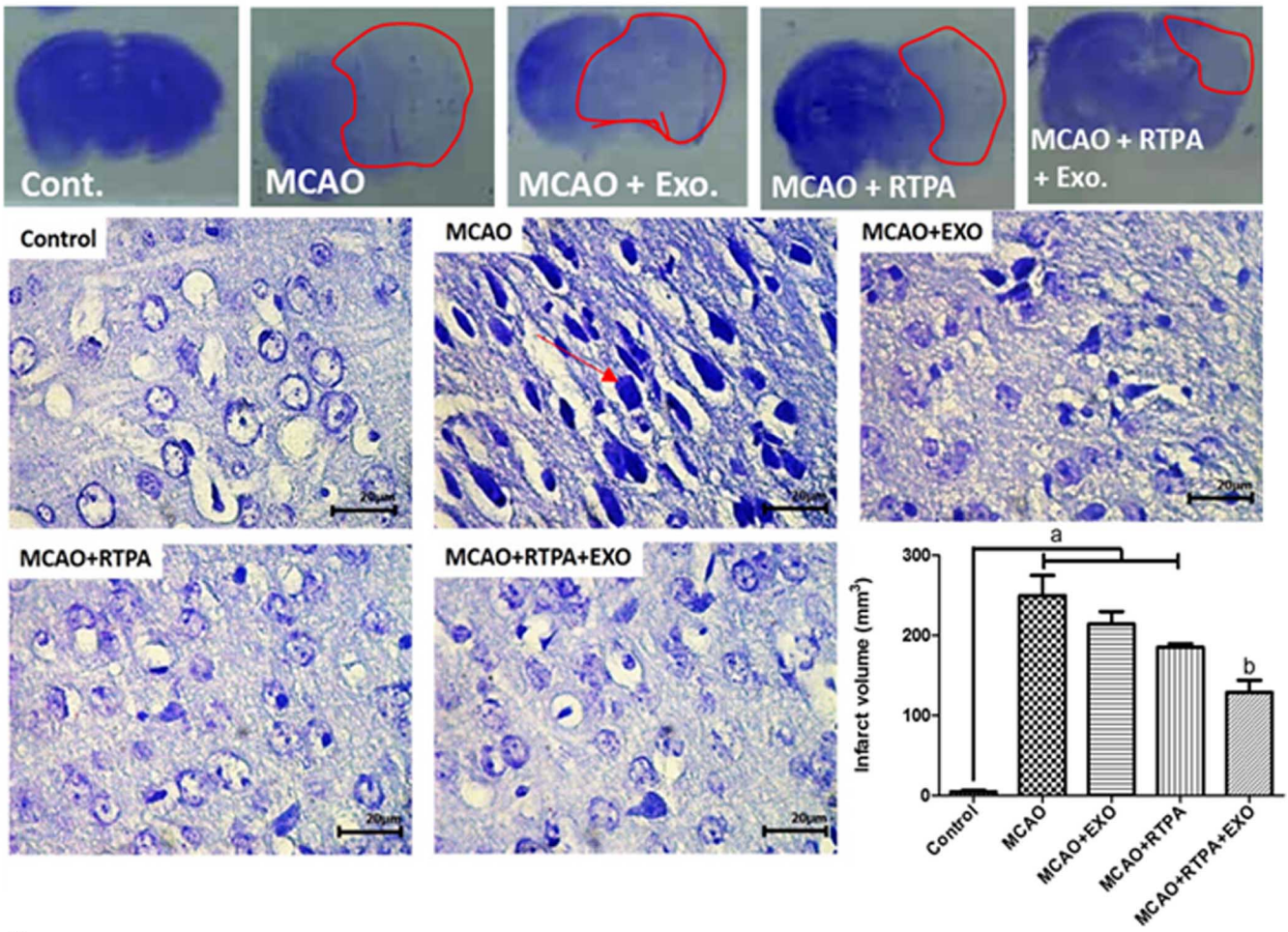

OPEN ACCESS and NO PUBLICATION FEE

http://dergipark.gov.tr/jcnos

Former name; Cell Membranes and Free Radical Research

Volume 15, Number 1, 2023

Journal of Cellular Neuroscience and Oxidative Stress

http://dergipark.gov.tr/jcnos

BSN Health Analyses, Innovation, Consultancy, Organization, Industry and Trade Limited Company

http://www.bsnsaglik.com.tr/

info@bsnsaglik.com.tr

Formerly known as:

Cell Membranes and Free Radical Research (2008 - 2014)

Volume 15, Number 1, 2023

[CONTENTS]

Volume 15, Number 1, 2023
E-ISSN Number: 2149-7222 (Online)
Indexing: Scopus (Elsevier), CAS (Chemical Abstracts Service), Citation Index Database, EBSCOhost Research Database, Google Scholar, Index Copernicus,

AIM AND SCOPES
Journal of Cellular Neuroscience and Oxidative Stress is an online journal that publishes original research articles, reviews and short reviews on the molecular basis of biophysical, physiological and pharmacological processes that regulate cellular function, and the control or alteration of these processes by the action of receptors, neurotransmitters, second messengers, cation, anions, drugs or disease.

Areas of particular interest are four topics. They are;

A- Ion Channels (Na^+- K^+ Channels, Cl^- channels, Ca^{2+} channels, ADP-Ribose and metabolism of NAD^+, Patch-Clamp applications)

B- Oxidative Stress (Antioxidant vitamins, antioxidant enzymes, metabolism of nitric oxide, oxidative stress, biophysics, biochemistry and physiology of free oxygen radicals)

C- Interaction Between Oxidative Stress and Ion Channels in Neuroscience
(Effects of the oxidative stress on the activation of the voltage sensitive cation channels, effect of ADP-Ribose and NAD^+ on activation of the cation channels which are sensitive to voltage, effect of the oxidative stress on activation of the TRP channels in neurodegenerative diseases such Parkinson's and Alzheimer's diseases)

D- Gene and Oxidative Stress
(Gene abnormalities. Interaction between gene and free radicals. Gene anomalies and iron. Role of radiation and cancer on gene polymorphism)

READERSHIP

Biophysics	Biochemistry
Biology	Biomedical Engineering
Pharmacology	PhysiologyGenetics
Cardiology	Neurology
Oncology	Psychiatry
Neuroscience	Neuropharmacology

Keywords
Ion channels, cell biochemistry, biophysics, calcium signaling, cellular function, cellular physiology, metabolism, apoptosis, lipid peroxidation, nitric oxide, ageing, antioxidants, neuropathy, traumatic brain injury, pain, spinal cord injury, Alzheimer's Disease, Parkinson's Disease.

RESEARCH ARTICLE

J Cell Neurosci Oxid Stress 2023;15(1): 1122-1136.

The treatment of exosome and recombinant tissue plasminogen activator reduces neuronal cell death in the middle cerebral artery occlusion stroke model of rats

Mohsen SAFAKHEIL[1], Mina RAMEZANI[1*], Azadeh MOHAMMADGHOLI[1]

[1]Department of Biology, Central Tehran Branch, Islamic Azad University, Tehran, Iran

Received: 21 March 2023; **Accepted:** 19 April 2023

***Address for correspondence:**

Mina RAMEZANI

Department of Biology, Faculty of Sciences, Central Tehran Branch, Islamic Azad University, Imam Hasan Boulevard, Ponak Square, Tehran, Iran Postal code:14676-86831

ORCID code: 0000-0002-9982-1276

Email: mina.ramezani@gmail.com

Phone: +989122238405

List of Abbreviations;

MCAO/R, *Middle cerebral artery occlusion/reperfusion;* ***rt-PA,*** *Recombinant tissue plasminogen activator;* ***NLRP,*** *NOD-like receptor protein;* ***EBST,*** *Elevated body swing test;* ***Pen-Strep,*** *penicillin-streptomycin*

Abstract

As brain stroke is one of the leading causes of death worldwide, in the current research neuroprotection and performance improvement have been investigated in the Middle cerebral artery occlusion/reperfusion (MCAO/R) animal model treated with exosomes combined with recombinant tissue plasminogen activator (rt-PA). MCAO/R was induced in 25 adult male Wistar rats. Rats received rt-PA (10 mg/kg, i.v.) or exosomes (100 µg/kg) derived from bone marrow mesenchymal stem cells (MSCs). Following the administration of rt-PA alone or in combination with exosomes, a significant increased score of the EBST test was recorded. Also, a decrease in error level of beam test was observed in the treated groups. Cresyl violet staining revealed that the population of dark cells was significantly reduced in all treated groups. The amount of catalase enzyme was significantly increased in all treated groups, especially in the combination therapy group ($P<0.05$). A considerable increase in superoxide dismutase (SOD) enzyme was observed in the combination therapy group compared to the MCAO/R group ($P\leq0.001$). Our conclusion was approved by the *Nlrp1* and *Nlrp3* downregulation during combination therapy in the MCAO/R model by a reduction in cell death rate. The density of GFAP-positive cells showed a significant decrease in the exosome with or without rt-PA- treated groups compared to the MCAO/R group ($P<0.05$). Our observation indicated that exosomes, in combination with rt-PA resulted in a noticeable functional recovery, neuronal

regeneration, and reduction of neuronal cell death after a 7-day period of the MCAO/R induction. This novel therapeutic strategy probably can provide a promising treatment for patients who suffered from a stroke.

Keywords: Neural regeneration, MCAO/R, Exosome, rt-PA, rat

Introduction

Brain stroke as the second reason of death is responsible for 1 of 9 deaths and many disabilities throughout the world and causes major adverse impacts in survivors (Kim et al., 2015; Allen and Buckberg, 2012). Approximately, 90% of all kinds of brain ischemia that are annually diagnosed in clinics are related to the arterial blockage. This type of disturbance resulted in narrowing or clotting of the blood vessels and cause the blood flow and oxygen level reduction, which leads to the death of neural cells (Hocum Stone et al., 2016). By attention to this proportion of stroke deaths, treatment strategies still need to be improved. The reperfusion methods such as prescribing thrombolytic medications or mechanical interventions can reanalyze the occluded vessels, facilitating the process of thrombolysis, which improves the treatment outcome after acute ischemic stroke (Savitz and Fisher et al., 2007). One of the available therapeutic tactics, which is useful only for the first 4.5 hours of the post-stroke period, is recombinant tissue plasminogen activator (rt-PA) as a thrombolytic agent (Hocum Stone et al., 2016). The administration of rt-PA is considered the gold standard treatment for acute ischemic stroke. This factor acts as a protease by which cleaves plasminogen and converts it into plasmin which, in turn, digests the fibrin clots, leading to the recanalization of the occluded vessels and maintenance of tissue homeostasis (Balami, et al., 2013). The neuroprotective effects of rt-PA have been also confirmed in middle cerebral artery occlusion (MCAO/R) animal models. However, it has been found that rt-PA administration can be effective only up to 4.5 hours after stroke. Thus, more applicable therapeutic strategies are required (Fluri, et al., 2015). Besides the administration of rt-PA, the newer therapeutic approaches based on cell replacement or the use of some secreting cell products are considered as promising therapeutic strategies for achieving more effective treatments. In this regard, stem cells and their secretions are one of the new strategies that have been revealed an effective outcome during an in vitro assessment. According to a previous study, the best time to use a cell therapy therapeutic approach is shortly after a stroke (Xin et al., 2013). Systemic management of MSCs, as a therapy for stroke, has demonstrated that MSCs are capable of enhancing the plasticity and neurovascular remodeling of the central nervous system (CNS), leading the improved neural functionality (Xin, Li and Chopp, 2014). These cells are able to change inflammatory reactions, oxidation components, and soluble cytokines secretion, and immune-modulatory receptors (Chen et al., 2003; Li et al., 2001; Lindvall and Kokaia, 2004). Exosomes are small-membraned vesicles with a diameter of 30 to 120 nm containing proteins, lipids, coding and non-coding RNAs (Vlasoo et al., 2012; Barteneva, et al., 2013) Cell secretions and molecular pathways inside and outside the cell are normally disrupted during a stroke. Therefore, following these changes, free radicals increase and an active immune system and destructive reactions will be induced in the body, especially in the brain tissue (Xin and Chopp, 2014; Zhang et al., 2015). Two types of inflammatory responses in reaction to ischemic stroke are NOD-like receptor protein 1 & 3 (NLRP1 & 3)-inflammasomes. It has been proposed that these sorts of mediate inflammatory responses increase IL-1 and IL-18 (Alishahi et al., 2019). It has been revealed that the exosomes derived from MSCs exhibited promising applications in regeneration medicine. The exosomes and other extracellular vesicles secreted from MSCs can promote the activation of the adaptive responses to tissue damages. It seems that the exosome does this by donating mitochondrial-related proteins which directly or indirectly up-regulate the antioxidant capacity of cells and regulating inflammatory responses such as the inflammasome at the cellular and molecular level. Thus, this study aimed to investigate the mechanism of synergistic effect of exosomes combination with rt-PA on inflammasome complex in the brain of the MCAO/R animal model.

Materials and Methods

Ethical issue

In this study, 25 male Wistar rats (250-300 g, 8-9 weeks age) were used, being kept under standard conditions with free access to food and water (45-50% humidity, 22-24 °C, 12 h: 12h light: dark cycle), were used. The methods used in the current research were conducted with adherence to the National Research Council's of

Health Guide for the Care and Use of Laboratory Animals (NIH).

Stem cell isolation and purification

Five animals were used for Bone marrow mesenchymal stem cells (BM-MSCs) isolation. BM-MSCs were isolated from the femur and tibia of the male Wistar rats and cultured in DMEM containing 10% fetal bovine serum (GIBCO; Germany) and 1% Pen-Strep (Li et al., 2018). The cells were characterized and passaged up to the 4th passage of cultivation at 37 °C, 5% CO2, and 95% humidity.

Exosome collection from BM-MSCs

Cell secretions were collected after each culture media replacement for 14 days, as described in our previous study (Safakheil and Safakheil., 2020). Briefly, the culture medium of the cells was centrifuged by ultra-high-speed centrifugation (2000×g for 10 min, 10,000×g for 30 min, and 100000×g for 60 min), (Pathakoti et al., 2018). Exosomes were investigated by western blot assessment for CD9 and CD81 membrane proteins. The exosomes were first isolated by electrophoresis of 6-12% polyacrylamide gel sulfate sodium dodecyl sulfate (SDS-PAGE). The PVDF membrane was used for transferring the protein and incubated for 12 hours at 4 °C along with CD9 and CD81 (Biorbyt Co., UK) and then HRP-conjugated secondary antibodies were applied to identify the protein markers. Protein blots were analyzed by luminol (Santa Cruz).

The characterization and morphological features of exosomes were evaluated using a scanning electron microscope (SEM, LEO 1430VP, Germany and UK). Furthermore, the average size and diameter of exosomes were determined by the dynamic light scattering (DLS) method using Zeta sizer Nano ZS (Malvern, UK).

Dil Labeling the exosomes

To ensure the exosome entrance into the central nervous system, exosomes were labeled by DiI (1,1′-Dioctadecyl-3,3,3′,3′-Tetramethylindocarbocyanine Perchlorate, Thermo Fisher Scientific, Waltham, MA) staining assay (Yi et al., 2020). For DiI labeling, 10 mg of DiI was added to the sample for 10 min. The staining was terminated by adding 10 mL PBS. Then exposed to DAPI (1/2000) for 10 min. The fluorescently labeled exosomes were visualized under a fluorescent microscope (Nikon, Japan).

Induction of the middle cerebral artery occlusion/reperfusion (MCAO/R) model

Twenty-five animals were anesthetized using the intraperitoneal injection of 8 mg/kg of xylazine and 100 mg/kg of ketamine**.** By making an incision in the midline of the neck under a surgical microscope, the right common carotid artery and the external and internal carotid arteries were exposed (Olympus Szx12, Germany). MCAO/R was induced in rats by inserting a silicone coat filament through the external carotid artery into the right internal carotid artery (Doccol Corp., Sharon, MA, USA). When it reached the anterior cerebral artery, the process was stopped (Sicard and Fisher, 2009). After 60 min, the filament was removed from the internal carotid.

Design of study

The animals were randomly divided into five groups (n = 5 per group) as (1) The normal group (Control), (2) The Ischemic group (MCAO/R), (3) The Ischemic group treated with exosome (MCAO/R + EXO), (4) The Ischemic group treated with an rt-PA group (MCAO/R + rt-PA), and (5) The Ischemic + Exosome + rt-PA group (MCAO/R + EXO + rt-PA). The exosomes were injected intravenously at 100 µg/kg for 7 days (Safakheil et al. 2020). Rt-PA (10 mg/kg) (Crumrine et al. 2011) was administered by intravenous injection immediately 4 h after MCAO/R induction for 7 days (Knecht et al. 2018).

Behavioral Assessments

The elevated body score test and beam test were employed as behavioral tests for the functional recovery assessment.

Elevated body swing test

To perform the analysis of the experimental stroke in rodents, the elevated body swing test (EBST) (Garcia test) was conducted by the method described by (Ingberg et al. 2015). The rats were placed in a clear cage and given two minutes to adjust to the environment and be in a neutral position (Set as having all four paws on the floor). Then, the animals were kept on a vertical axis so that they could not deviate more than 10 degrees on either side. The oscillation was marked each time. The animal moves its head off the vertical axis to the right or left. Animals that do not have any brain lesions turn their heads evenly in

both directions, but animals that have brain lesions on one side of their brain, such as ischemic stroke, are expected to present a dominant/biased swing direction (Ingberg et al. 2015).

Beam test

The Ledged Beam test is used to assess motor balance in rodent models of CNS disorders. In this test, the mice were trained to walk across an elevated beam that gradually narrows in width as they reach a safe platform. The beam had a ledge that catches the animal's paw if it slips off the edge (Alibut et al. 2007). Misplacements of the paw off the beam were video-recorded and scored.

Cresyl violet staining

Cresyl violet staining was applied to evaluate the cell death rate in the brain tissues. After separating the brains from the skull of rats, the tissues were fixed overnight. The brain samples were dehydrated by alcohols series with increasing concentration, then they were washed using xylene, and infiltrated with paraffin. The paraffin-embedded specimens were coronally sectioned with a thickness of 5 μm (Licka, USA). The slices were then placed on slides and stained with purple 2% Cresyl after clearing and rehydration. The samples were then covered with enthlan adhesive and the stained slides were visualized under a light microscope with a magnification of 400 (Labomed, the USA). After imaging the slides, the cells around the peri-infarct were counted by the ImageJ software (version 1.8, NIH, Wayne Rasband, and the USA). Cell shrinkage, cytoplasm, loss of Nissl body uniformity, pycnotic nucleus, nucleus density, and also infarct volume in the damaged brain tissues were assessed by light microscopy (Labomed, the USA).

Real-time PCR

Total RNA was extracted from 100 mg of brain tissue using Qiazol (Qiazol lysis reagent, the USA) in sterilized RNase-free tubes. The Revert aid cDNA synthesis kit (Fermentas, Germany) in a volume of 25 μL was used, according to the manufacturer's recommendations. The Primer3 software was used to design the primers and then the primers (**Table 1**) were approved by the NCBI BLAST Tool. 500 ng of synthesized cDNA was used for the analysis of the relative gene expression by real-time PCR. PCR reactions were carried out in a total volume of 25 μL containing 12.5 μL of SYBR Green Premix 2X (Takara, Shiga, Japan) and 10 pico-molars of mixed primers. Thermocycling conditions were as the following setting: 95 °C for 10 sec, followed by 40 cycles of denaturation at 94 °C for 5 sec, annealing and extension at 60 °C for 34 sec. To determine the expression of the relative expressions for the *Nlrp1 and Nlrp-3* genes, the $2^{-\Delta\Delta CT}$ method was used. The obtained CTs were compared for both the internal control (*Gapdh*) and the samples.

Western blot

The protein concentration of the brain tissue extract was determined by the Bradford method (Bio-Rad Protein Assay, Hercules, CA, the USA). Protein samples (50 mg/lane) were separated on a 10% SDS polyacrylamide gel electrophoresis (SDS-PAGE) with a constant voltage of 75 V. The electrophoresed proteins were further transferred to polyvinylidene difluoride (PVDF) membrane (Millipore, Bedford, MA, 0.45 mm pore size) with a transfer apparatus (Bio-rad). Primary antibodies including the Nlrp1 (Cat No. sc-390133), Nlrp3 (Cat No. sc-518123) and Gapdh (Cat No. sc-47724) (Santa Cruz Biotechnology, Santa Cruz, CA, the USA).

Table 1. *Primer sequence of Nlrp1 and Nlrp3 genes*

gene	Forward	Reverse	Accession number	Product length
Nlrp3	5′ GGAGTGGATAGGTTTGCTGG 3′	5′ GGTGTAGGGTCTGTTGAGGT 3′	XM_006246458.3	163 bp
Gapdh	5′ AAG TTC AAC GGC ACA GTC AAG G 3′	5′ CAT ACT CAG CAC CAG CAT CAC C 3′	XM_017593963.1	121 bp
Nlrp1	5′ CAAGAGGGAAAGGTGGACAG 3′	5′ GGAAGTGATGGGGATGAAGTGT 3′	XM_006246755.3	183 bp

The immunoblots were washed three times in TBS buffer for 10 min and then immersed in the second antibody solution containing goat anti-mouse IgG-HRP and goat anti-rabbit IgG-HRP (Cat No. sc-525387, Santa Cruz) for 1 h and diluted 500-fold in TBS buffer. The immunoblots were then washed in TBS buffer for 10 min three times. The immunoblotted protein levels were visualized using an enhanced chemiluminescence ECL western blotting luminal Reagent (Santa Cruz, CA, USA) and quantified using a Fujifilm LAS-3000 chemiluminescence detection system (Tokyo, Japan).

Immunohistochemistry

Immunohistochemical analysis was performed for detecting GFAP (astrocyte marker) and IBA1(microglia marker) positive cells. The 5 μm-sectioned brain samples were rehydrated and then incubated in phosphate buffer for 100 min at 100 °C, then the samples were washed with phosphate buffer (PBS), The blocking process was performed for 30 minutes with 0.4% Triton X-100 in PBS and goat serum (10%). In the next step, the sections were incubated with the primary antibody against GFAP (Abcam, Cambridge, the United Kingdom) and IBA1 (Abcam, Cambridge, the United Kingdom) at the dilution ratio of 1:100 at 4 °C for overnight. Then, the slides were incubated at 37 °C for 90 minutes with Peroxidase-conjugated secondary antibodies. Finally, by performing a 3, 3'-diaminobenzidine tetrahydrochloride (DAB) reaction, the GFAP or IBA1-positive cells were visualized. The nuclei were stained with hematoxylin. The samples were then viewed under a light microscope (Labomed, the USA) at 400X magnification. Then the expression of GFAP and IBA1 in neuronal cells was assessed using the Image J software.

Terminal deoxynucleotidyl transferase-mediated dUTP nick end labeling (TUNEL) assay

To measure the DNA fragmentation, In situ cell death detection method was performed with POD Kit (Roche, Germany). First, the histological sections were incubated whit proteinase K (15 μg/ml) for half an hour. In order to block the endogenous peroxidase activity, the samples were incubated in the dark for 10 min at room temperature whit 3% hydrogen peroxide/methanol.

The samples were then washed 3 times each time for 5 min with Tris buffer, then Incubation with the tunnel reaction mixture was performed on the sections for 1 hour at 37 ° C.

DAPI solution was then used as counterstain. After that, the sections were washed three times and each time for 5 minutes with Tris buffer, and then the number of TUNEL positive neurons in 3 sections of the peri-infarct area of the cortex per animal was carefully counted. The percentage of positive cells against total nuclei was calculated using the Image J software v1.8 (NIH, Wayne Rasband, and the USA).

Superoxide dismutase activity and the Catalase levels

Using a microplate assay kit (Padtangostar Co, Iran), Superoxide dismutase activity (SOD) and Catalase levels during one week after ischemia was calculated according to the recommended protocol. The hemispheres of the brain with ischemia were homogenized, then 10 μl of sample poured into each well of a microplate and incubated in the assay solution. Also 10 μL of normal saline was added as blank (control) in a well. All samples and solutions should be at ambient temperature. The rest of the steps were done according to the kit's instructions.

The kit uses a xanthine oxide reagent at room temperature. This substance generates superoxide in the presence of oxygen that converts a colorless substrate to a yellow color product. By increasing the levels of enzyme in the sample, a decrease in superoxide concentration and yellow color occurs. Then, the optical density was calculated using an ELISA reader (EX800, the USA) at 450 nm (OD 450) for 20 min (Kashani et al. 2021). Using serial dilutions, the slope of the standard curve was calculated to determine the sample concentration. The kit’s sensitivity was equal to 0.044 U/mL.

Statistical analysis

The GraphPad Prism version 7.04 was used to analyze the data. To compare the differences between the experimental groups, One-way analysis of variance (ANOVA) was considered followed by Tukey's post hoc test. Data were obtained as mean ± standard error (SE) and data considered significant when the P-value was less than 0.05.

Results

Exosome characterization

The surface markers on isolated particles were characterized by western blotting to confirm CD9 and CD81 expression. These are the conserved biomarkers and

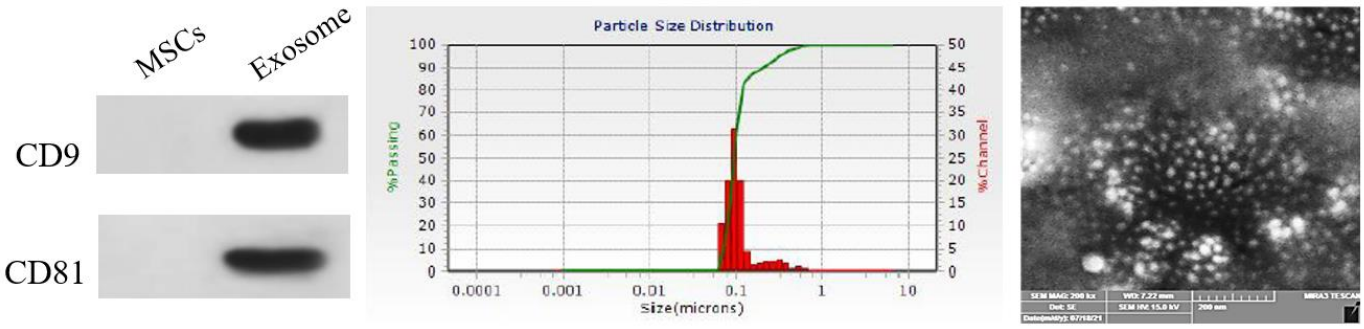

Figure 1. *Characterization of MSC-derived exosomes. Western blot analysis of the exosomal surface markers CD9, CD81. Mesenchymal stem cells (MSCs) secrete exosomes in environmental cell culture and themselves did no reaction to specific markers for exosomes (Left). DLS analysis showed that the size of exosomes was approximately 100 nm (Middle). SEM image of exosomes (Right).*

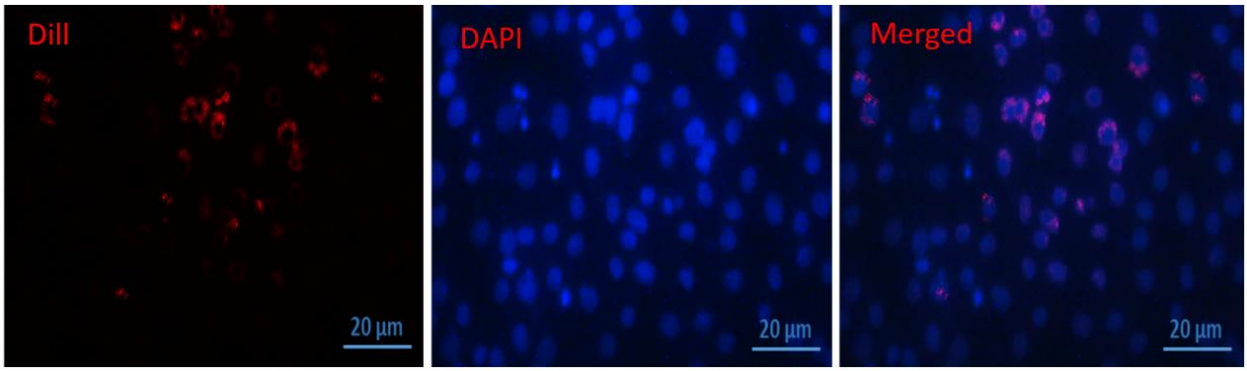

Figure 2. *Tracking of MSC-derived exosomes by DiI labeling. For DiI labeling, 10 mg of DiI was added to the sample for 10 min, then exposed to DAPI (1/2000) for 10 min. Distribution of DiI dye (red) in the cytoplasm of the cell around nucleus stained by DAPI (blue). Magnification: ×400*

are widely used for exosome characterization (**Figure 1**). The result showed that exosomes contained CD9 and CD81 markers on their surface. DLS analysis also showed that the size of exosomes was around 100 nm. This size and SEM image of exosomes confirmed that exosomes were collected rightly during exosome extraction.

Exosome tracking analysis

Confirmation of exosomes entrance into the central nervous system was investigated by DiI labeling. The results showed that exosomes have been penetrated into neural and glial cells 7 days after treatment in exosome-treated groups (**Figure 2**).

Behavioral test

Elevated body swing test (EBST)

In this test, the ratio of rat rotation on the left (the healthy part of the brain) to the right (the damaged part of the brain) was examined. This ratio equaled to 1 indicates the healthy control group. Compared to the control group, a significantly reduced ratio was observed in MCAO and MCAO+EXO groups. Following the administration of rt-PA alone or in combination with exosomes, an increased score of the EBST test was recorded that was significant in comparison to MCAO and MCAO+EXO groups and non-significant comparing to the control group (**Figure 3**).

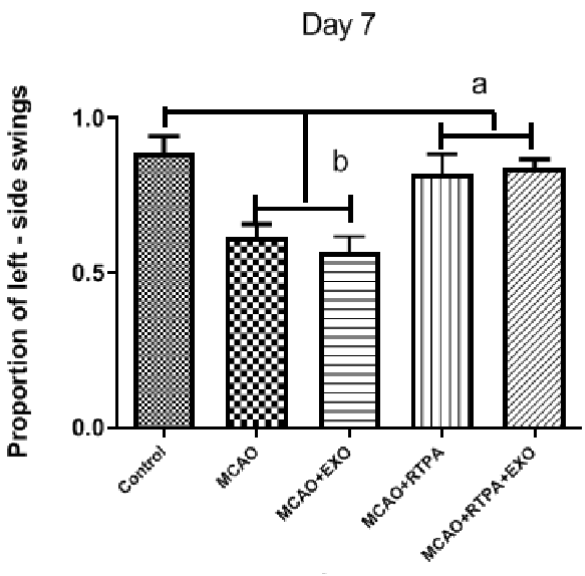

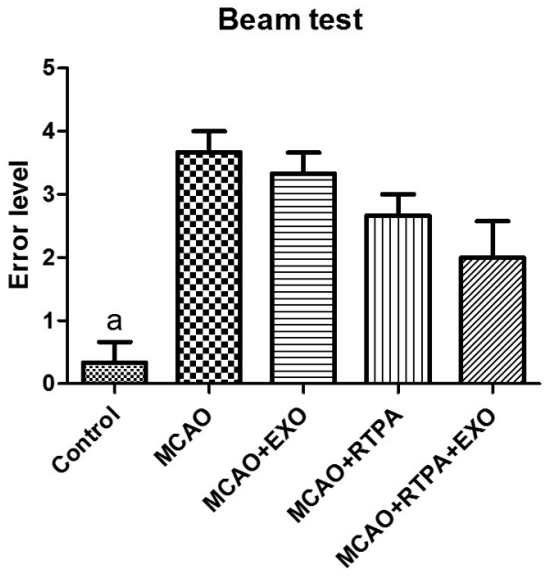

Figure 3*. Evaluation of the EBST test score in different experimental groups in 7 days. Values are expressed as the means and standard error of the mean (mean ± SEM), (n=5 per group). Means corresponding to bars not sharing any letter are significantly different at (P<0.05). MCAO/R: middle cerebral artery occlusion, EXO: exosomes, RTPA: recombinant tissue plasminogen activator.*

Figure 4*. Evaluation of sensorimotor deficits in different experimental groups in 7 days. Misplacements of the paw off the beam were scored in each animal. Values are expressed as the means and standard error of the mean (mean ± SEM), (n=5 per group). a: significant difference between the control and experimental groups (P<0.05). There was no significant difference between the experimental groups. MCAO/R: middle cerebral artery occlusion, EXO: exosomes, RTPA: recombinant tissue plasminogen activator.*

Ledged Beam Test

In the beam test, the motor coordination and movement balance were assessed in the untreated and the treated MCAO/R models. It was observed that control healthy mice were able to pass through the beam without any slipping. The error rate was significantly increased in MCAO/R models. After treatments with exosomes and rt-PA alone or in the combined form, a decrease in error level was observed in the MCAO/R+EXO, MCAO/R+rt-PA, and MCAO/R+EXO+ rt-PA groups. However, the observed decrease of error level was not statistically significant (**Figure 4**).

Cresyl violet staining

As shown in **Figure 5**, Cresyl violet staining was employed to identify the apoptotic cells in brain tissue of MCAO/R induced rats after 1 week of model induction. The highest quantity of inky cells of neural tissues (81% ±3.46) was detected in the MCAO/R group by a semi-quantitative method in comparison with the other groups. The percentage of the cells died through apoptosis in the MCAO/R+EXO, MCAO/R+RTPA and MCAO/R+RTPA+EXO groups was respectively (39.33±0.88), (31.67±1.33) and (26 ±1.52). The death percentage in the MCAO/R+RTPA+EXO group was remarkably (P <0.05) lower than the MCAO/R group.

Exosomes and rt-PA effects on transcriptional levels of *Nlrp3 and Nlrp1*

The expression of the *Nlrp3 and Nlrp1* genes was quantified to identify the degree of inflammation in the brain tissue of rats before and seven days after MCAO/R

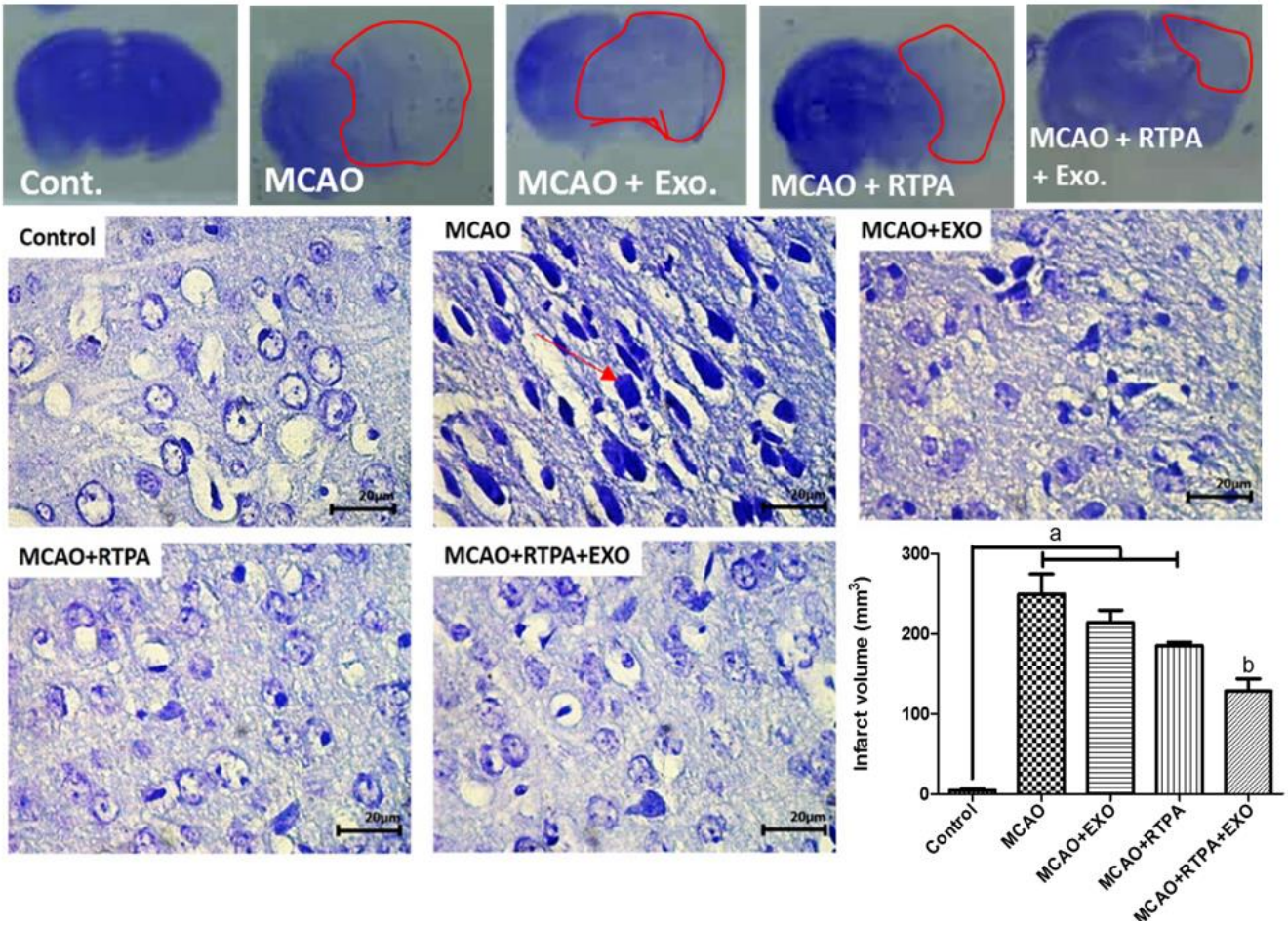

Figure 5. *Representative of the penumbral cortex of ischemic hemisphere stained with Cresyl violet stain seven days after the onest of MCAO/R in all groups. The dead cells are indicated by the arrow. Infarct volume in the damaged hemisphere of the brain showed an increase of pale surface of the brain after MCAO induction. The obtained data are represented as the means and standard error of the mean (mean ± SEM). a & b.; represent statistically significant differences between the other experimental groups in the mean values (P<0.05). MCAO/R: middle cerebral artery occlusion, EXO: exosomes, RTPA: recombinant tissue plasminogen activator. Scale bars: 20 µm.*

induction. According to **figure 5**, the levels of *Nlrp3 and Nlrp1* genes expression in the MCAO/R group were noticeably higher in comparison with the other groups. The monotherapy of either exosome or rt-PA causes to downregulation of the expression of the *Nlrp3 and Nlrp1* genes in comparison with the MCAO/R group ($p<0.05$). The combined exposure therapy with exosome and rt-PA cause to reduce the levels of *Nlrp3 and Nlrp1* genes expression in the MCAO/R+RTPA+EXO group in comparison with other investigational groups ($p < 0.05$) (**Figure 6**).

Nlrp3 and Nlrp1 protein expression

The increased changes in Nlrp3 and Nlrp1 proteins in the MACO groups compared to the control group indicated the induction of the inflammation in the brain tissue and an increased apoptosis signaling. Impact of rt-PA and exosomes on the expression of the Nlrp3 and Nlrp1 after 7 days of MCAO induction revealed a reduction in both protein expression compared to the MCAO group. Down-regulation of these two factors was observed in the exosome and rt-PA groups compared to the MCAO group (**Fig. 7**).

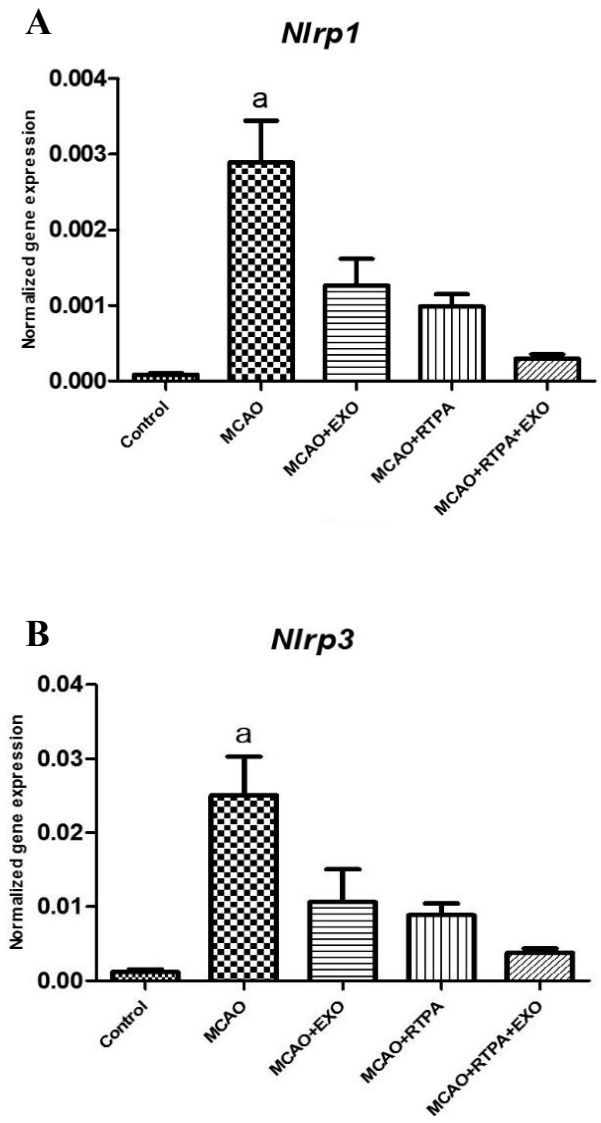

Figure 6*. The impact of rt-PA and exosomes on the expression of the (A) Nlrp1 and (B) Nlrp3 genes measured by the real-time PCR analysis in the brain tissue of rats 7 days after MCAO/R induction. The transcriptional level of each sample was normalized against the expression of Gapdh. The reactions were performed in six separate experiments. a.; represents statistically significant differences between the other experimental groups in the mean values (P<0.05). MCAO/R: middle cerebral artery occlusion, EXO: exosomes, RTPA: recombinant tissue plasminogen activator.*

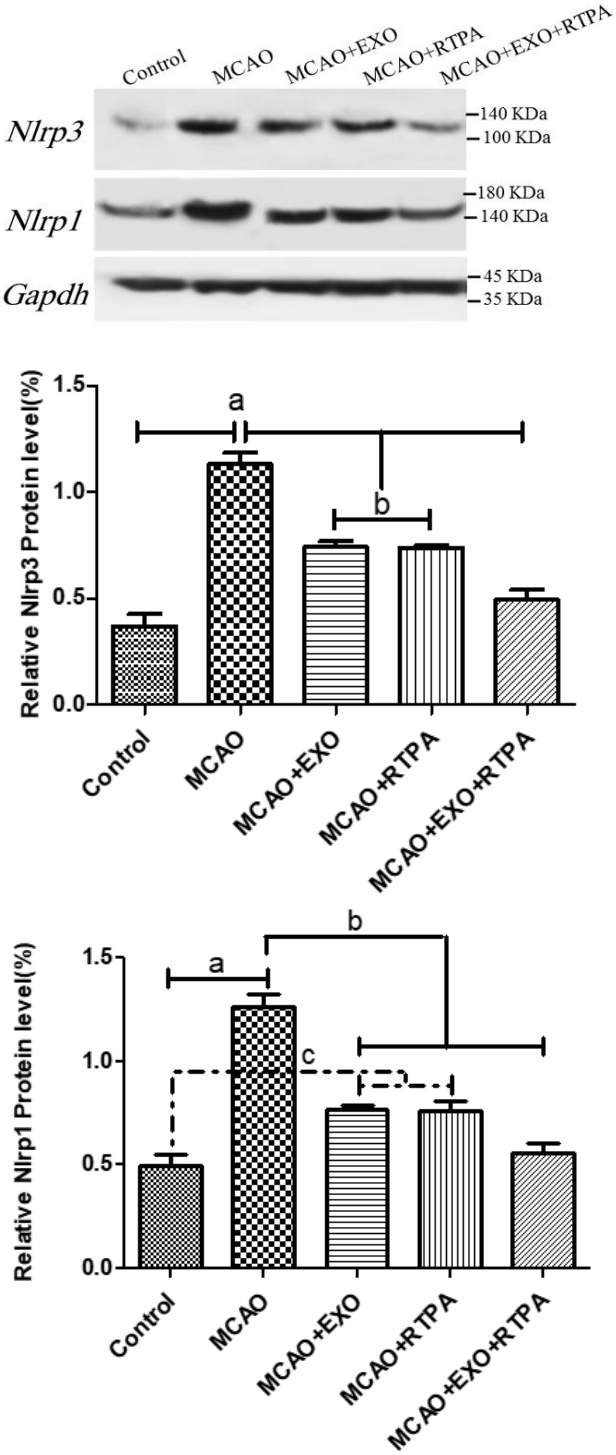

Figure 7*. Western blot analysis of Nlrp3 and Nlrp1 protein expression in the studied groups in comparison with the control group. This is a cropped figure; full-length blot is presented in Supplementary Figure [II]. Gapdh was used to confirm the normalization of the protein load. RTPA with Exosome had significant effects on expression levels of Nlrp3 and Nlrp1 protein compared to the MCAO group. a, b & c.; represent statistically significant differences between the other experimental groups in the mean values (P<0.05).*

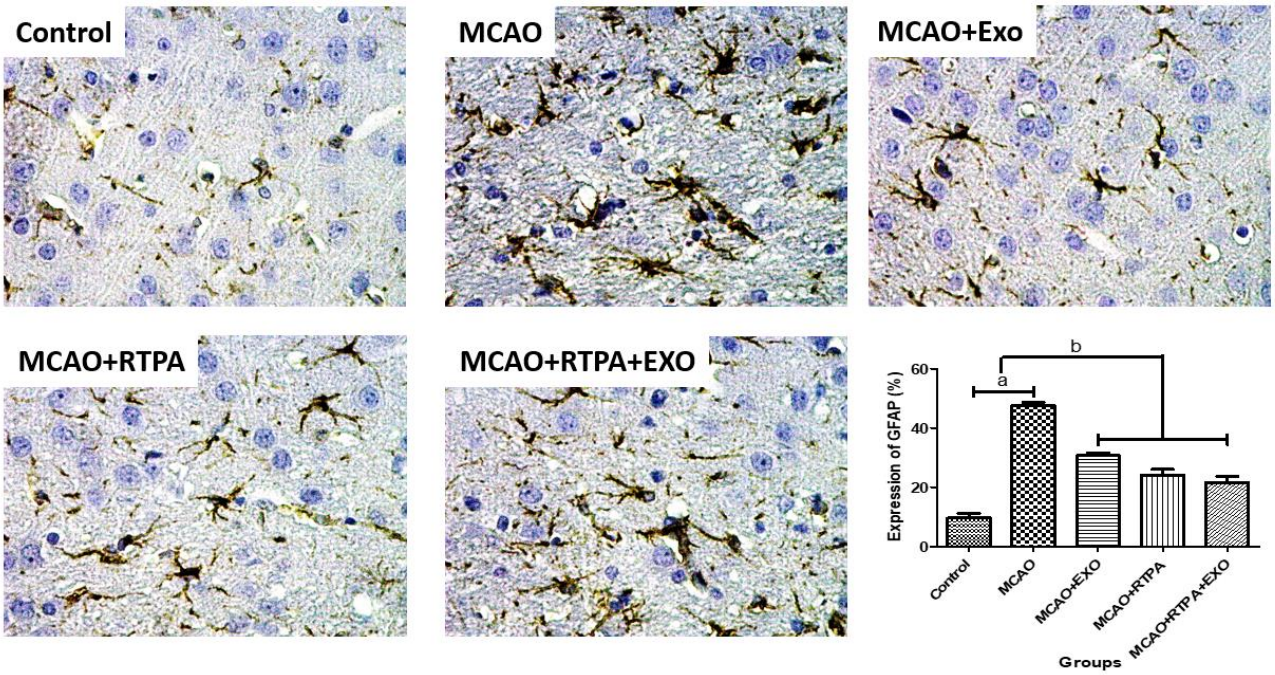

Figure 8. *Immunohistochemical analysis of the GFAP-positive cells (astrocytes) in the cortex of the brain tissue of rats 7 days after MCAO/R induction in different experimental groups. The arrow shows the GFAP-positive cells. Data represent means±SE of three experiments. a & b.; represent statistically significant differences between the other experimental groups in the mean values (P<0.05). MCAO/R: middle cerebral artery occlusion, EXO: exosomes, RTPA: recombinant tissue plasminogen activator Scale bars: 20 µm.*

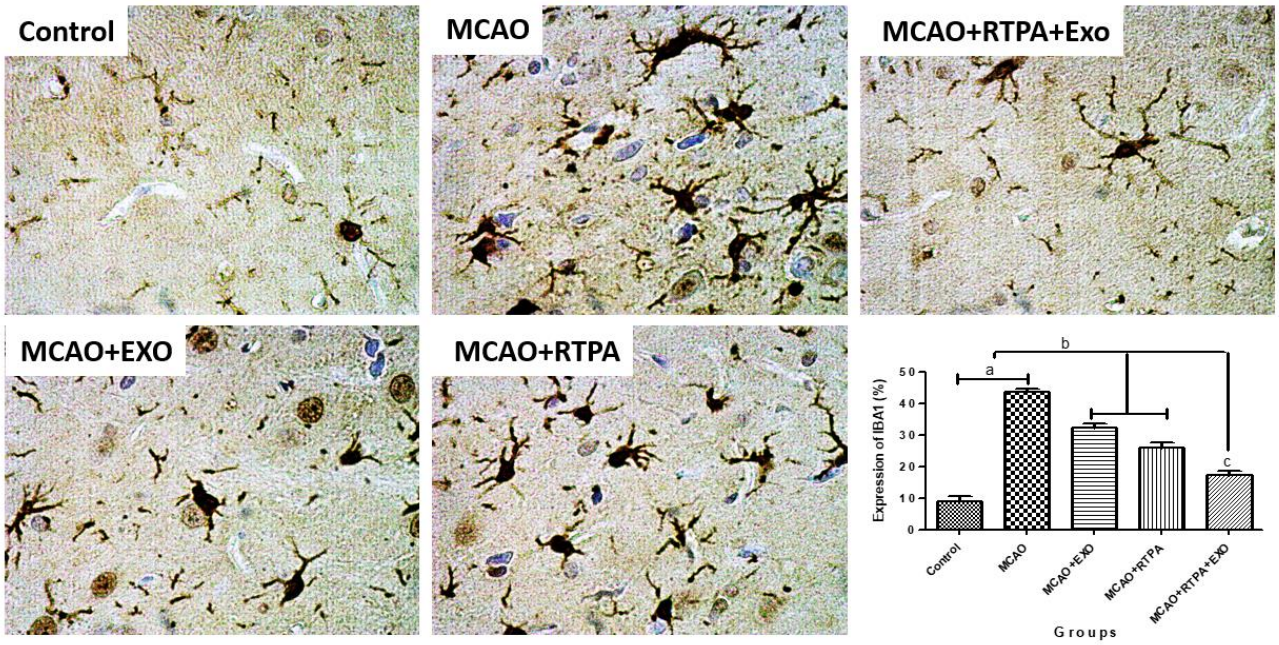

Figure 9. *The expression of IBA1 (microglia marker) in the cortex of the brain tissue of rats 7 days after MCAO/R induction in different experimental groups. Data represent means±SE of three experiments. a, b & c.; represent statistically significant differences between the other experimental groups in the mean values (P<0.05), (n=5 per group). Data represent means ± SE of three experiments. MCAO/R: middle cerebral artery occlusion, EXO: exosomes, RTPA: recombinant tissue plasminogen activator. Scale bars: 20 µm*

GFAP and IBA1 Expression

The Glial fibrillary acidic protein (GFAP) expressing cells (**Figure 8**) were detected by the immunohistochemical analysis following the MCAO/R induction, and the positive cell percent was measured in all investigational groups. The highest percentage (47.47 % ± 1.14) of GFAP expressing cells was detected in the MCAO/R group (**Figure 8**) in comparison with other investigational groups. The GFAP expressing cell percent in the MCAO/R+EXO (30.62% ± 0.9) and MCAO/R+rt-PA groups (24% ± 2.08) was remarkably decreased in comparison to the MCAO/R group ($p \leq 0.05$). No significant difference was observed between the MCAO/R+EXO and MCAO/R+ rt-PA groups. In the MCAO/R+EXO+ RTPA group, the percent of GFAP expressing cells was remarkably ($p \leq 0.05$) lessen to 21.67%± 2.02.

Ionized calcium-binding adaptor molecule 1 (IBA1) protein expression was shown in **Figure 9** that measured with the IHC method. Similar to GFAP and histopathological changes of the brain tissue, the highest expression of IBA1 protein belonged to the MCAO/R group and the therapeutic intervention cause to decrease significantly in IBA1 compared with the MCAO/R group ($p \leq 0.05$). Investigation of the effect of each therapeutic intervention revealed that IBA1 expression in MCAO/R + RTPA + EXO group decreased significantly in comparison with the MCAO/R + EXO and control ($p = 0.001$).

TUNEL assay

According to **Figure 10** A&B, MCAO/R increased the apoptotic cells in the brain ($p = 0.001$ compared to the control group). It was also found that the greatest decrease in apoptotic cells was in the MCAO/R + RTPA + EXO group.

Superoxide dismutase activity and the Catalase levels

Changes in antioxidant enzymes were evaluated by SOD and Catalase measurements (**Figure 11**, A&B). The results of this study showed a significant decrease of SOD values in the rat brain tissue with MCAO/R compared to the control group ($p = 0.001$). However, only the MCAO/R + RTPA + EXO group showed a significant increase compared to the MCAO/R group ($p = 0.001$) and the observed changes in other groups were not significant (**Figure 8A**). However, all therapeutic interventions were able to increase catalase activity compared to the MCAO/R group ($p \leq 0.05$). The largest increase was observed in the MCAO/R + EXO + rt-PA group (**Figure 11B**).

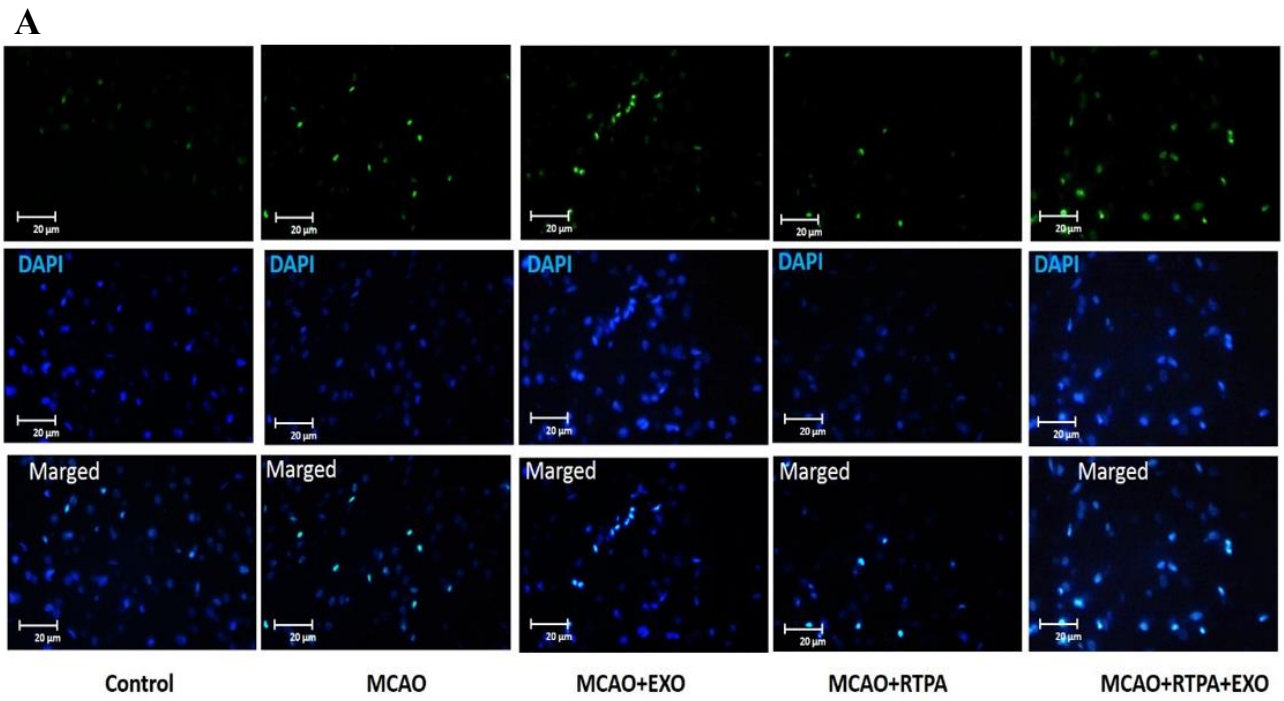

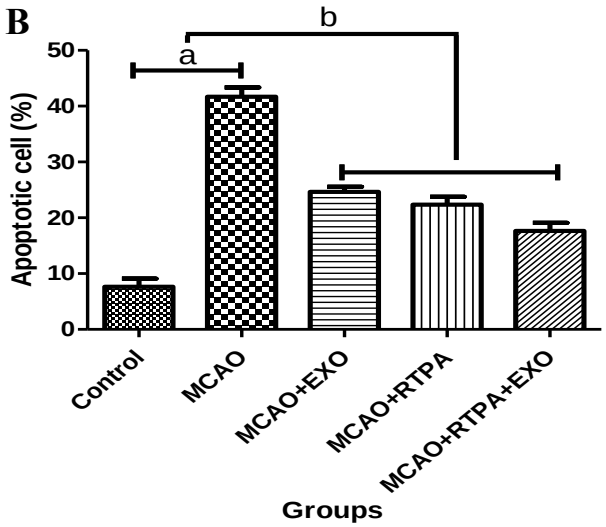

Figure 10. *Apoptotic cells in different groups by TUNEL assay (A&B). A: TUNEL positive neurons stained by green color (top row), Nuclei of cells stained by Dapi blue color (middle row), combination of both protein expression and nucleus staining (bottom row). a & b.; represent statistically significant differences between the other experimental groups in the mean values (P<0.05). Data represent means ± SE of three experiments. MCAO/R: middle cerebral artery occlusion, EXO: exosomes, RTPA: recombinant tissue plasminogen activator.*

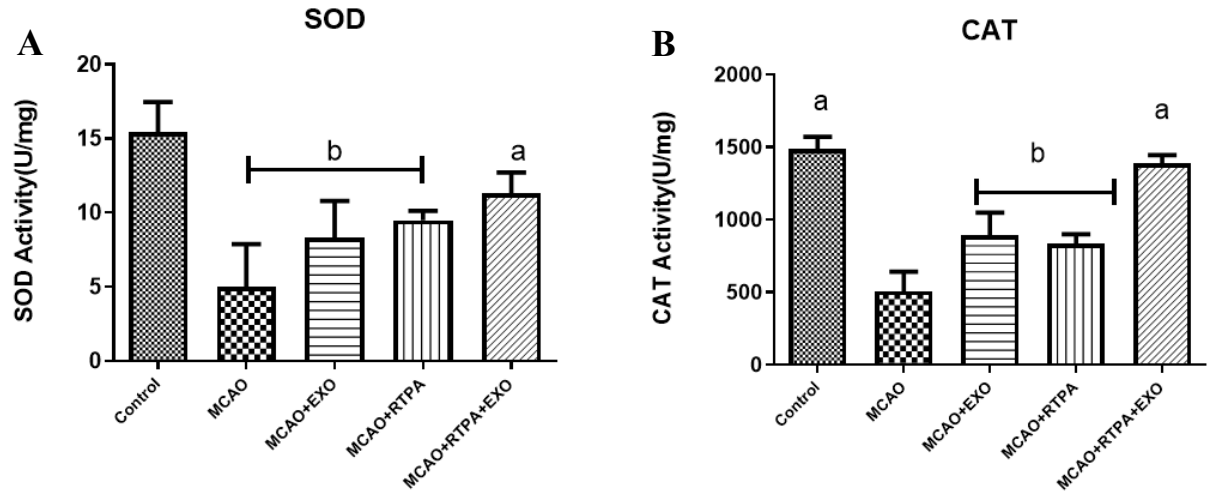

Figure 11. *Changes of SOD and Catalase levels in the five groups (A&B). Data represent means ± SE of three experiments). Means corresponding to bars not sharing any letter are significantly different at (P<0.05). MCAO/R: middle cerebral artery occlusion, EXO: exosomes, RTPA: recombinant tissue plasminogen activator.*

Discussion

In spite of various therapies for the protection and recovery of neuronal tissues following the stroke induction, the long-term disabilities would be persistent due to the severe side effects and narrow therapeutic time window (Savitz and Fisher, 2007). Many therapeutic approaches have failed to show a treatment protocol for the complete recovery of neurological functions. Recombinant tissue plasminogen activator (rt-PA) is the only Food and Drug Administration (FDA)-approved drug for the mitigation of stroke, and it is considered the standard therapeutic regimen for post-stroke patients but it would be effective only if administered at the first hours of stroke incidence. In this regard, rt-PA was given to animal models four hours after stroke onset. The blood-brain barrier can cause limitations for some chemical agents to gain access to the CNS; therefore, many neurological diseases are deprived of effective drugs to be able to penetrate the BBB and enter the target site. Considering this critical issue, nanocarriers are increasingly being designed and developed to be capable of crossing the BBB and serving as a drug delivery system. Nowadays, stem cells have evolved a unique source for the secretion of exosomes, which are considered natural nano-vesicles in biologically active molecules. Exosomes act as paracrine effectors that easily interrelate the cells and cross the selective-permeable membranes such as BBB, thus emerging as a multipurpose tool for some therapeutic strategies (Zagreen et al. 2018). Therefore, in the present study, as a novel therapeutic vehicle, we investigated the neuroprotective effect of exosomes in combination with rt-PA on rats induced by MCAO/R. Furthermore, to minimize some side effects of rt-PA administration such as promoting the leucocyte infiltration and inflammation (Yang et al. 2019), cell-derived exosomes having neuroprotective effects were applied as a promising therapy. In this research, the bone marrow mesenchymal stem cells-derived exosomes were applied as a neuroprotective agent alone or in combination with rt-PA. According to our data, the Garcia grading system represented the sensory and movement-related neuronal activity of the rat brain which showed significant enhancement following the combined exposure therapy with exosome and rt-PA after one week of MCAO/R induction. Although the administration of each compound enhanced Garcia's score, however, the difference between the treatment groups and the MCAO/R group was not significant. In line with our study, Xin et al., for the first time, examined the therapeutic efficiency of exosomes derived from MSCs in rats induced by MCAO/R. They demonstrated that the functional recovery occurred in response to treatment with exosomes (Xin et al. 2013). Exosomes contain miRNA, siRNA, cytosolic, and some membrane proteins such as enzymes, growth factors, receptors, and cytokines (Thery et al. 2001). Accordingly, exosomes derived from MSCs have been shown to alter the gene expression and promote brain recovery by changing the miRNA profile expression (Liu et al. 2013). MSCs and exosomes both have the ability to increase neurite remodeling, neurogenesis, and angiogenesis (Xin et al., 2014). Our findings showed that apoptotic cells, which were remarkably increased in the MCAO/R group, were decreased in the rats receiving exosomes alone or in combination with rt-PA, denoting the neuroregenerative and neuroprotective potential of exosomes in MCOA/R models. Regarding the resulting data, it could be suggested that exosome treatment reduces the apoptosis rate of neuronal cells in the brain of MCAO models by downregulating the expression of NLRP1 and NLRP3 inflammasomes and their downstream targets including caspase1. It has been recognized that inflammasome signaling pathways, particularly NLRP3, mediate inflammation induction following cell injuries or some pathological conditions like stroke and subsequently promote the cell death pathway in neurons and glial cells (Feng et al. 2020). On the other hand, MSCs-derived exosomes have exhibited to play a neuroprotective role in cell or tissue injuries occurred in either central nervous system or spinal cord, by inhibiting pro-inflammatory factors and modulating the intracellular defense mechanisms including vitagene networks and anti-inflammatory responses (Calabrese et al. 2010; Chen, et al., 2018). Moreover, our data demonstrated that the number of the GFAP expressing cells (astrocytes) and IBA-1 expressing cells (microgelia) was remarkably decreased in the brain of rats receiving exosome/rt-PA or a combination of both. These cells will be activated in response to different pathological stimuli such as stroke, inflammation, trauma, and ischemia. GFAP is usually an index of neural damage or gliosis and IBA1 is upregulated during the activation of microglia (brain resident macrophage) (Yu et al. 2018). Consistently, our results clearly demonstrated the increase of IBA-1 and GFAP-expressing cells in MCAO/R models. Thus, it seems that rt-PA/exosome treatment could modulate the immune

responses in the brain. rt-PA can reanalyze the clogged vessels and enhance neuronal survival through the digestion of fibrin clots, facilitating the performance of exosomes at the site of tissue damage. Several lines of evidence indicated the beneficial effect of MSCs on neuronal functions in patients who are post-stroke (Chen, et al., 2018; Knecht, et al., 2018). Wang et al. examined the impact of bone marrow MSCs on rats that underwent spontaneous intracerebral hemorrhage. They showed that intravenously transplanted bone marrow MSCs exert beneficial effects on rats that were induced by stroke. Also, Han et al. identified more than 2000 proteins in exosomes, which are derived from MSCs, that many of them were involved in the brain repair process (Han et al. 2018). Although exosomes derived from different cells can exert neuroprotection, those derived from MSCs can also reduce inflammation and enhance angiogenesis and neurogenesis after the onest of stroke (Chen, et al., 2018). Likewise, consistent with our study, Zhang et al., for the first time, depicted that MSCs derived exosomes promote the practical recovery after brain lesion via enhancing angiogenesis and neurogenesis and they indicated that exosomes were considered as a competent therapy to reduce inflammation in rats after the onset of infarction (Zhang et al. 2015). Our observation of Cresyl violet staining also confirmed reduction of Infarct volume in the brain after 7 days of administration of rt-PA/exosome and specially their combination in MCAO/R rats. Moreover, the activity of antioxidant enzymes such as Cat and SOD increased by rt-PA/exosome treatment. Studies have shown that increasing the activity of Cat and SOD reduces programmed cell death, activates astrocytes and microglia, and releases anti-inflammatory elements (Fujimura et al. 1999). It has been reported that exosomes can play an anti-oxidative stress role in neurodegenerative diseases by themselves (Xia et al. 2021). However, the mechanism underlying changes of oxidoreductase enzymes by exosomes have not been clarified.

In the current study, we presented a novel therapeutic strategy in which MSCs-derived exosomes, in combination with rt-PA, were employed for the enhancement of neurogenesis in rats immediately after MCAO/R induction. The fidelity of the current approach is due to (1) the breakdown of clogged arteries mediated by rt-PA and (2) the ability of nano-sized exosomes to pass through the BBB, leading to the efficient delivery of miRNA, growth factors, and multiple proteins and enzymes effective in the reduction of inflammation, promotion of neurogenesis and angiogenesis in the injured neural tissues.

Conclusion

In conclusion, the usage of exosomes accompany with rt-PA resulted in the promotion of functional recovery, neuroprotective activity enhancement, and keeping the cells viable due to neuroinflammatory reduction effect in rats after 7 days of MCAO/R induction.

Acknowledgements

We would like to thank central Tehran Branch, Islamic Azad University for their kindly laboratory support.

Conflict of interests

The authors declare that they have no conflicts of interest.

Funding

No supportive fund was received for conducting this study.

Authors' contributions

All Authors did idea designing, data collection, and data analysis; Mohsen Safakheil performed the experiments and wrote the draft; Mina Ramezani and Azadeh Mohammadgholi edited the manuscript and did data analysis. All Authors read and approved the manuscript.

Declaration of Conflicting Interests

The author declared no potential conflicts of interest with respect to the research, authorship, and/or publication of this article.

Ethics approval

The experimental protocols were conducted with adherence to the International Council for Laboratory Animal Science (ICLAS) and approved by the ethical committee of Tehran Islamic Azad University of Medical Sciences (IR.IAU.TMU.REC.1398.091). Consent to participate is not applicable.

References

Alishahi, M., Farzaneh, M., Ghaedrahmati, F., Nejabatdoust, A., Sarkaki. A., & Khoshnam, S.E. (2019). NLRP3 inflammasome in ischemic stroke: As possible therapeutic target. Int J Stroke, 14, 574-591.

Allbut,t H.N., & Henderson, J.M. (2007). Use of the narrow beam test in the rat, 6-hydroxydopamine model of Parkinson's disease. Journal of neuroscience methods. 30;159(2):195-202.

Allen, B. S., & Buckberg, G. D. (2012). Studies of isolated global brain ischaemia: I. Overview of irreversible brain injury and evolution of a new concept–redefining the time of brain death. Eur Journal Cardiothorac Surg, *41*(5), 1132-1137.

Balami, J. S., Sutherland, B. A., & Buchan, A. M. (2013). Complications associated with recombinant tissue plasminogen activator therapy for acute ischaemic stroke. CNS Neurol Disord Drug, *12*(2), 155-

169.

Barteneva, N. S., Maltsev, N., & Vorobjev, I. A. (2013). Microvesicles and intercellular communication in the context of parasitism. Front Cell Infect Microbiol , *3*, 49.

Calabrese, V., Cornelius, C., Dinkova-Kostova, A. T., Calabrese, E. J., & Mattson, M. P. (2010). Cellular stress responses, the hormesis paradigm, and vitagenes: novel targets for therapeutic intervention in neurodegenerative disorders. Antioxid Redox Signal, *13*(11), 1763-1811.

Chen J, & Chopp M. (2018) Exosome Therapy for Stroke. Stroke. 49:1083-1090.

Chen, J., Li, Y., Katakowski, M., Chen, X., Wang, L., Lu, D., . & Chopp, M. (2003). Intravenous bone marrow stromal cell therapy reduces apoptosis and promotes endogenous cell proliferation after stroke in female rat. J Neuroscience Research, *73*(6), 778-786.7.

Crumrine, RC., Marder, VJ., Taylor, GM., LaManna, JC., Tsipis CP., .& Arora V. (2011). Intra-arterial administration of recombinant tissue-type plasminogen activator (rt-PA) causes more intracranial bleeding than does intravenous rt-PA in a transient rat middle cerebral artery occlusion model. Exp Trans Stroke Med, 3(1):1-4.

Feng, Y. S., Tan, Z. X., Wang, M. M., Xing, Y., Dong, F., & Zhang, F. (2020). Inhibition of NLRP3 inflammasome: A prospective target for the treatment of ischemic stroke. Front Cell Neurosci, *14*, 155.

Fluri, F., Schuhmann, M. K., & Kleinschnitz, C. (2015). Animal models of ischemic stroke and their application in clinical research. Drug Des Devel Ther, *9*, 3445.

Fujimura, M., Gasche, Y., Morita-Fujimura, Y., Massengale, J., Kawase, M., & Chan, PH. (1999). Early appearance of activated matrix metalloproteinase-9 and blood–brain barrier disruption in mice after focal cerebral ischemia and reperfusion. Brain research, 18;842(1):92-100.

Hocum Stone, L. L. H., Xiao, F., Rotschafer, J., Nan, Z., Juliano, M., Sanberg, C. D., ... & Low, W. C. (2016). Amelioration of ischemic brain injury in rats with human umbilical cord blood stem cells: mechanisms of action. Cell Transplant, *25*(8), 1473-1488.

Ingberg E, Gudjonsdottir J, Theodorsson E, Theodorsson A, & Ström JO. Elevated body swing test after focal cerebral ischemia in rodents: methodological considerations. BMC Neurosci 2015; 16:50.

Kashani, M.H., Ramezani, M & Piravar, Z., (2021). The effect of acrylamide on sperm oxidative stress, total antioxidant levels, tyrosine phosphorylation, and carboxymethyl-lysine expression: A laboratory study. Inter J Rep Bio Med, 19(7), 625.

Kim, Y. D., Cha, M. J., Kim, J., Lee, D. H., Lee, H. S., Nam, C. M., . & Heo, J. H. (2015). Long-term mortality in patients with coexisting potential causes of ischemic stroke. Inter J Stroke, *10*(4), 541-546.

Knecht, T., Borlongan, C., & dela Peña, I. (2018). Combination therapy for ischemic stroke: Novel approaches to lengthen therapeutic window of tissue plasminogen activator. Brain Circ, *4*(3), 99.

Li, Y., Chen, J., Wang, L., Lu, M., & Chopp, M. (2001). Treatment of stroke in rat with intracarotid administration of marrow stromal cells. Neurology, *56*(12), 1666-1672.

Li, C., Wang, F., Zhang, R., Qiao, P., & Liu, H., (2020). Comparison of proliferation and osteogenic differentiation potential of rat mandibular and femoral bone marrow mesenchymal stem cells in vitro. Stem Cells Dev, 1;29(11):728-36.

Nudo, R. J., & Duncan, P. W. (2004). Recovery and rehabilitation in stroke: introduction. Stroke, *35*(11_suppl_1), 2690-2690.

Liu, F. J., Lim, K. Y., Kaur, P., Sepramaniam, S., Armugam, A., Wong, P. T. H., & Jeyaseelan, K. (2013). microRNAs involved in regulating spontaneous recovery in embolic stroke model. PloS one, *8*(6), e66393.

Han Y, Seyfried D, Meng Y, Yang D, Schultz L, Chopp M, & Seyfried D. (2018) Multipotent mesenchymal stromal cell–derived exosomes improve functional recovery after experimental intracerebral hemorrhage in the rat. J Neurosurg, 20;131(1):290-300.

Pathakoti, K., Manubolu, M., & Hwang, H. M. (2018). Nanotechnology applications for environmental industry. In Handbook of nanomaterials for industrial applications Elsevier. pp. 894-907.

Safakheil, M., & Safakheil, H. (2020). The effect of exosomes derived from bone marrow stem cells in combination with rosuvastatin on functional recovery and neuroprotection in rats after ischemic stroke. J Mol Neurosci, *70*(5), 724-737.

Savitz, S. I., & Fisher, M. (2007). Future of neuroprotection for acute stroke: in the aftermath of the SAINT trials. Ann Neurol, *61*(5), 396-402.

Sicard, K. M., & Fisher, M. (2009). Animal models of focal brain ischemia. Exp Transl Stroke Med., *1*(1), 1-6.

Théry, C., Boussac, M., Véron, P., Ricciardi-Castagnoli, P., Raposo, G., Garin, J., & Amigorena, S. (2001). Proteomic analysis of dendritic cell-derived exosomes: a secreted subcellular compartment distinct from apoptotic vesicles. J Immunol, *166*(12), 7309-7318.

Vlassov, A. V., Magdaleno, S., Setterquist, R., & Conrad, R. (2012). Exosomes: current knowledge of their composition, biological functions, and diagnostic and therapeutic potentials. Biochim Biophys Acta, *1820*(7), 940-948.

Xia, C., Dai, Z., Jin, Y., & Chen, P. (2021) Emerging antioxidant paradigm of mesenchymal stem cell-derived exosome therapy. Front Endocrinol,1523.

Xin, H., Li, Y., & Chopp, M. (2014). Exosomes/miRNAs as mediating cell-based therapy of stroke. Front Cell Neurosci, *8*, 377.

Xin, H., Li, Y., Liu, Z., Wang, X., Shang, X., Cui, Y., ... & Chopp, M. (2013). MiR-133b promotes neural plasticity and functional recovery after treatment of stroke with multipotent mesenchymal stromal cells in rats via transfer of exosome-enriched extracellular particles. Stem cells, *31*(12), 2737-2746.

Yang, E., Cai, Y., Yao, X., Liu, J., Wang, Q., Jin, W., ... & Wu, J. (2019). Tissue plasminogen activator disrupts the blood-brain barrier through increasing the inflammatory response mediated by pericytes after cerebral ischemia. Aging (Albany NY), 11(22), 10167.

Yi, YW., Lee, JH., Kim, SY., Pack, CG., Ha, DH., Park, SR.,.& Cho, BS. (2020). Advances in analysis of biodistribution of exosomes by molecular imaging. Int J Mol Sci. 2020 Jan 19;21(2):665.

Yu, X., Wang, X., Zeng, S., & Tuo, X. (2018). Protective effects of primary neural stem cell treatment in ischemic stroke models. Exp Ther Med, *16*(3), 2219-2228.

Zagrean, A. M., Hermann, D. M., Opris, I., Zagrean, L., & Popa-Wagner, A. (2018). Multicellular crosstalk between exosomes and the neurovascular unit after cerebral ischemia. Therapeutic implications. Front Neurosci, *12*, 811.

Zhang, Y., Chopp, M., Meng, Y., Katakowski, M., Xin, H., Mahmood, A., & Xiong, Y. (2015). Effect of exosomes derived from multipluripotent mesenchymal stromal cells on functional recovery and neurovascular plasticity in rats after traumatic brain injury. J Neurosurg, *122*(4), 856-867.